Association of Metallurgical Engineers of Serbia *Scientific paper*
AMES *UDC: 669.295.5'71'292.018.8 ; 621.794.6*

COMPARATIVE STUDY ON BIOACTIVE COATING OF Ti-6Al-4V ALLOY AND 316 L STAINLESS STEEL

Sajjad Jafari[1], Mehdi Mazar Atabaki [1,2*], Jamaliah Idris[1]

[1]*Department of Materials Engineering, Faculty of Mechanical Engineering, Universiti Teknologi Malaysia, 81310, Malaysia*
[2]*Institute for Materials Research, the School of Process, Environmental and Materials Engineering, Faculty of Engineering, University of Leeds, Leeds, LS9 2JT UK*

Received 13.10.2011
Accepted 23.12.2011

Abstract

In the present investigation, hydroxyapatite (HA) bioactive coating is deposited with sol-gel method on the surface of 316 L stainless steel and Ti-6Al-4V alloy as the most important biomaterials. Biocompatible additives such as P2O5, Na2CO3, KH2PO4 and HA commercial powder have been used for preparation of HA sol-gel. Characterization of the coated specimens was performed using SEM, XRD, EDS, AFM and optical microscopy. Substrates mechanical properties, e.g. micro hardness and bonding strength, were evaluated in respect to the substrates sintering temperature after completion of the coating process. The results show that denser structure of HA can be obtained by increasing the sintering temperature. In addition, pores volume fraction and size decreased by increasing the sintering temperature. It is shown that surface roughness of the HA decreased when the sintering temperature was incresed to 800 °C. However, growth of the HA grains for the coated alloys sintered at 800 ºC is attributed to the slight increase in roughness. Hardness and bonding strength of the biomaterials increased for the metals sintered at the higher temperatures. Different responses to the mechanical tests have been seen for in the titanium alloy sintered at 800 °C.

Keywords: Hydroxyapatite; Titanium alloy; Stainless steel; Sol-gel coating

Introduction

Metals, polymers, ceramics and composites are being vastly employed to replace bones in surgery of the damaged parts. Among the various materials available in the market, metallic biomaterials like titanium alloys and stainless steels are widely used for the implant surgery applications due to their good corrosion resistance and mechanical

* Corresponding author: Mehdi Mazar Atabaki ,pmmmaa@leeds.ac.uk.

properties. There are many reports in improving the bioactive coatings, as well as the enormous use of hydroxyapatite (HA) on the surface of the biomaterials [1-4]. Hydroxyapatite (Ca10(PO4)6(OH)2) is one of the most prominent biocompatible ceramic materials which promotes osseointegeration of implant materials to surrounding tissue due to its similar composition and structure to the human body [5-7]. Osseointegeration is defined as structural connection between implant surface and surrounding tissue [8]. Different methods of bioactive coating deposition on the surface of metallic biomaterials have been reported, such as plasma spraying [9-11], sputtering [12,13] and electrophoretic deposition [14-17]. It has been reported that a thick non-uniform coating and low bonding strength between coating layer and substrate are the result of the different coating techniques [16,18]. However, sol-gel technique is a simple and cheap method with producing high purity and homogenized coatings for high purity and uniform coating deposition for high purity and uniform coating deposition. Synthesis of HA through sol-gel method was extensively discussed in the literature [19-24]. To our knowledge, there are not sufficient studies on high production rate and coating of the implant materials by applying a simple method. Aksakal et al. [25] observed a cracked surface for HA thick coatings, e.g. more than 20 μm, and average bonding strength of 20 MPa was reported. The problem of long surface crack appearance in thick coating is also addressed by other researchers [17]. Therefore, this study is trying to compare different properties and characterization of HA coating on two metallic biomaterials (Ti-6Al-4V alloy and 316L stainless steel) in the same condition. In addition, HA powders along with biocompatible additives were used in order to produce HA coatings with thickness of 10-50 μm. Surface coatings, free from cracks, are obtained for both substrates. The surface morphology and chemical composition of the deposited coatings have been evaluated using scanning electron microscopy (SEM), energy dispersive X-ray spectroscopy (EDS) and X-ray diffraction analysis (XRD). Atomic force microscopy (AFM) has been utilized to better understand the effect of sintering temperature on the HA coating surface morphology.

Experimental procedure

To produce HA gel, 0.01 mole HA (HCa5O13P3) was hydrolyzed in 1.3M ethanol solution followed by vigorous stirring for 24 h. Afterwards, P2O5 with the molar ratio of 10, Na2Co3 with molar ratio of 2 and small amount of KH2PO4 were added to the HA sol. During mixing of the chemical additives, ultrasonic treatment was used in order to increase the homogeneity of the gel. In order to examine the chemical reactions, occurring during sol-gel preparation, differential thermal analysis and thermal gravimetry analysis (DTA/TG) were performed from 50 ºC to 800 ºC with a heating rate of 10 K min-1 for HA gel. The titanium alloy and stainless steel specimens were machined into cylinders with 10 mm in diameter and 2 mm in length. After machining, the specimens were ground up to 1200 grit paper, cleaned in alcohol followed by ultrasonic bath cleaning in acetone. Afterwards, specimens were passivated in nitric acid (40%) for 45 minutes. The substrates were coated using various dipping rate and withdrawal rate ranging from 5 to 10 cm/min. At this stage, the specimens were sintered in a vacuum furnace at 600, 700 and 800 °C. The heating rate during the final sintering process was 5 °C/min. Corrosion behavior of the passivated metallic biomaterials was examined using electrochemical measurements in simulated body solution (pH=7.37) at 37 °C. All of the tests were conducted using a Parstat-2263 potentiostat/galvanostat

according to the ASTM G-5 standard. Graphite and saturated calomel electrode (SCE) were used as counter and reference electrode, respectively. Titanium alloy and stainless steel plates, 10×20×20 mm in size, were prepared using the wire cut machine in order to evaluate bonding strength of the HA coating. Pull-out test was performed at a cross speed of 1 mm/min using Instron mechanical testing machine. Microhardness of the deposited coating layers was estimated by applying 300 g load for 15 s. Three tests were performed for each specimen to verify the results. The surface morphology and composition of the coatings were analyzed using scanning electron microscopy (SEM), energy dispersive spectroscopy (EDS) and X-ray diffractometry (XRD). Surface topography and roughness of the HA coatings were investigated by atomic force microscopy (AFM) operated in tapping mode. SEM examinations were performed with a JEOL Scanning Electron microscope (JSM-5200, Japan) with a beam voltage of 20Kv. X-ray diffraction pattern for HA powder and HA coating were recorded in a Philips Ph-1730 X-ray crystallographic unit provided with a proportional counter. The probe in the AFM (cantilever) was oscillated at or near its resonant frequency. The oscillating probe tip was then scanned at a height where it barely touched the sample surface. The system was monitored the probe position and vibrational amplitude to obtain topographical and other property information. Optimum resolution was about 50 Å lateral and <1 Å height.

Results and discussion

DTA/TG results

TG and DTA data of the HA gel are shown in Fig. 1. The first endothermic peak, which appears at 120 ºC, is due to evaporation of the absorbed water and ethanol. Appearance of the second endothermic peak at about 160 °C confirmed the crystallization of the HA, while appearance of the third endothermic peak at 240 °C points out to removal of the chemical additives. The TG graph, presented in Fig. 1b, shows a total weight loss of 44% during heat treatment, including the evaporation of the absorbed water, removal of the additives and crystallization of HA.

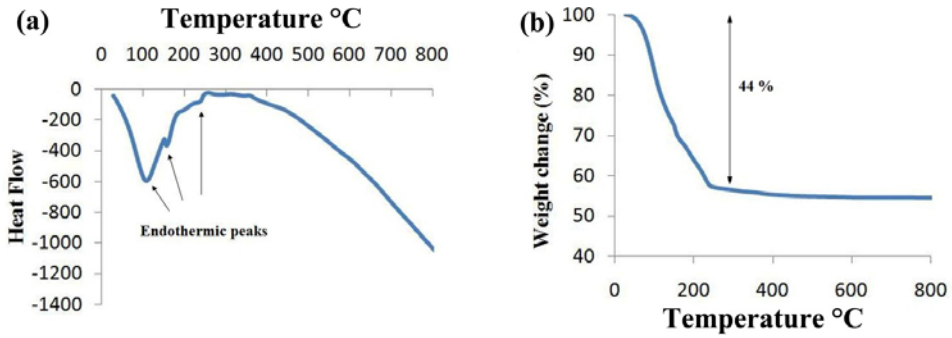

Fig.1. Results of (a) DTA and (b) TG analysis of HA gel in the temperature range from 50 ºC to 800 ºC.

Corrosion measurements

Electrochemical corrosion examination of titanium alloy and stainless steel samples showed that corrosion current of the titanium alloy is about 2.271e-001 μA, while corrosion current of the stainless steel is around 2.389e+001 μA. Corrosion potential of the titanium alloy and the stainless steel stood at about -537.6 mV and -323.1 mV, respectively. By considering the graphs, it is clear that Ti-6Al-4V shows different electrochemical behaviour in simulated body environment during electrochemical tests. The titanium alloy, during the entire test, showed an active to passive transition behavior. After passivating of both substrates in nitric acid, electrochemical tests were conducted once again and following results were obtained. The corrosion currents of the titanium alloy and the stainless steel specimens are respectively decreased to 1.333e-002 μA and 3.592e-001 μA, verifying improvement in corrosion resistance of both alloys. This can be explained by the formation of a protective layer consisted of TiO_2 and Cr_2O_3 at the surfaces of the examined materials.

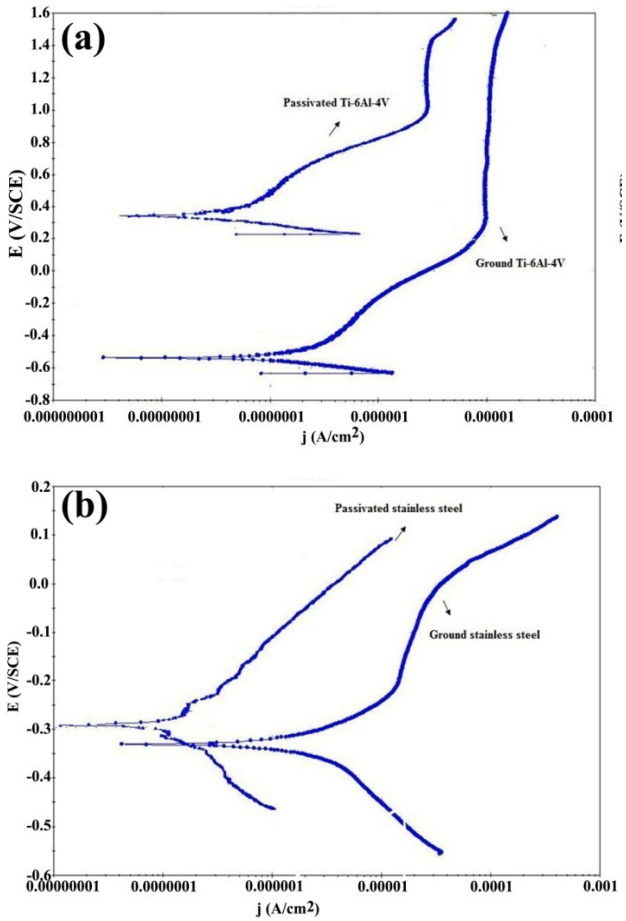

Fig.2. Polarization curves of (a) Ti-6Al-4V alloy and (b) 316L stainless steel in simulated body solution at 37 °C.

Characterization of HA layer

Appearance of the long cracks on the coating surface, even after drying of the specimens in air was completed, can be attributed to the hydrogen evolution. Presence of these cracks at the coating layer surface may lead to failure of the coating layer. To overcome this problem, influence of different coating deposition parameters, such as coating thickness and amount of chemical additives, were investigated. Fig.3 shows the cracked surface of HA layer deposited on the surface of examined biomaterials after the drying process.

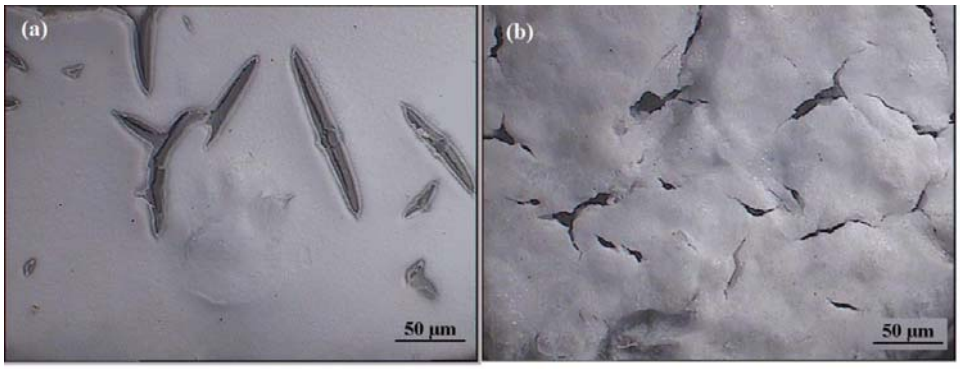

Fig.3. SEM micrographs showing cracked surface of HA layer deposited on the surface of (a) 316L stainless steel and (b) Ti-6Al-4V alloy specimens.

Surface morphology of deposited HA coatings, sintered at three different temperatures, is shown in Fig.4. HA coating deposited on the surface of 316 L stainless steel and Ti-6Al-4V alloy sintered at 600 °C showed a porous structure free from any cracks (see Figs. 4(a) and (d)). Other researchers reported that open interconnected porous structure is of a great interest since it enables penetration of the tissue cells and helps in prevention of loosening and movement of the implant, thus enhancing biointegration and mechanical stability of the implant/bone interface [26, 27]. It is shown that by increasing the sintering temperature the denser HA structure can be obtained. Sintered HA coating, deposited on the stainless steel surface does not show presence of any cracks at 800 °C, while at the surface of HA coating deposited on the titanium alloy presence of the numerous cracks can be observed after sintering at 800 °C (Fig. 4 (f)). As it can be seen from Fig.4, with increasing the sintering temperature the amount of pores are decreased and to some extent the number of the cracks are increased on the surface of both alloys. However, as the crystallinity of the HA coatings at the higher sintering temperatures is improved, the cracks are appeared to become wider on the surface of the titanium alloy. Large dents produced on the deposited surface of the alloys. These cavities act as reservoirs for the sol solution during dip coating and therefore these thicker-coated areas are more susceptible to cracking due to excessive drying and sintering strain. The surface features of the grooves and cavities with irregular geometry appear to be replicated by the coating deposition.

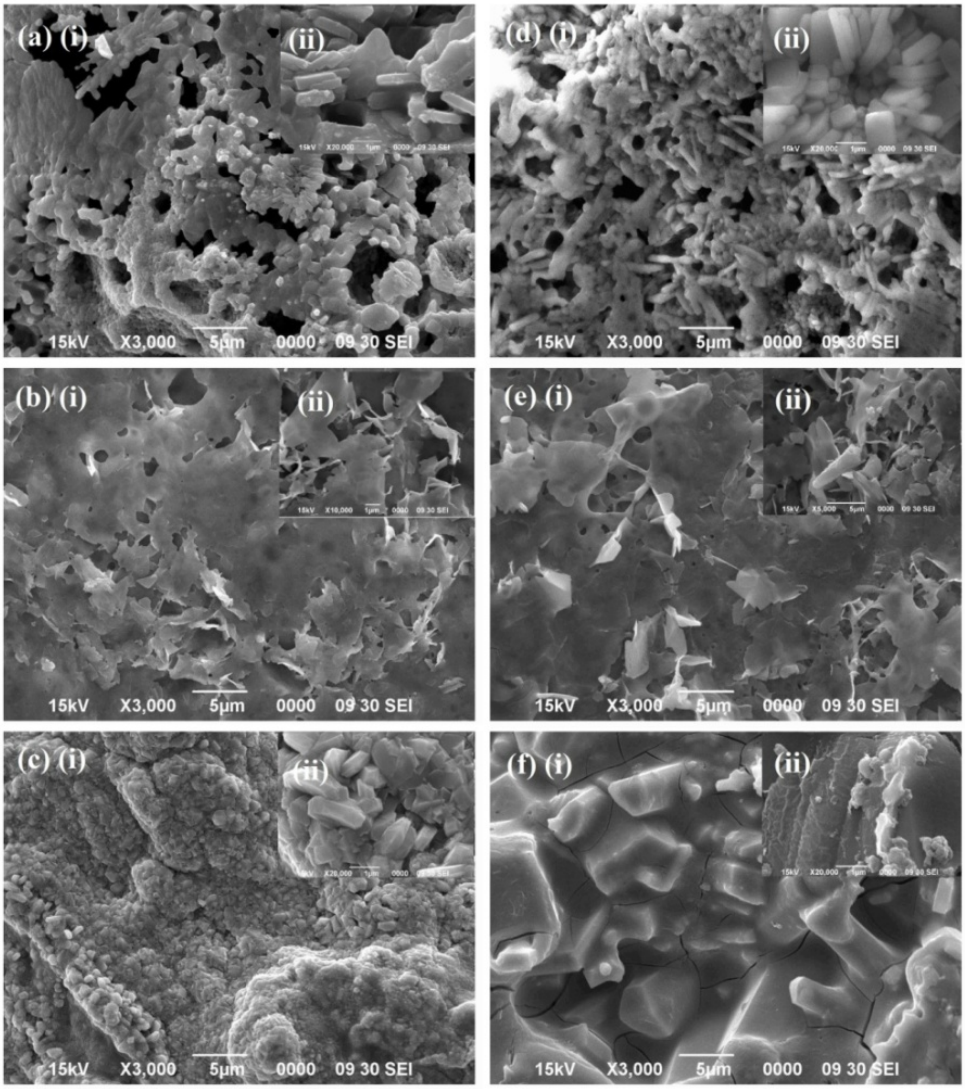

Fig.4. SEM micrographs of HA coating deposited on the surface of 316 L stainless steel sintered at a) 600 °C, b) 700 °C, c) 800 °C and Ti-6Al-4V alloy sintered at d) 600 °C, e) 700 °C, f) 800 °C. Note: i and ii indicate different magnification of the micrographs.

The sintering process transform the amorphous phase into crystalline HA and the microstructure of the coatings are shown to be dependent on the sintering temperature. Mapping analysis of the HA coating deposited on the 316L stainless steel surface revealed presence of oxygen, phosphorous, calcium, carbon and sodium as surface contaminants (see Fig. 5).

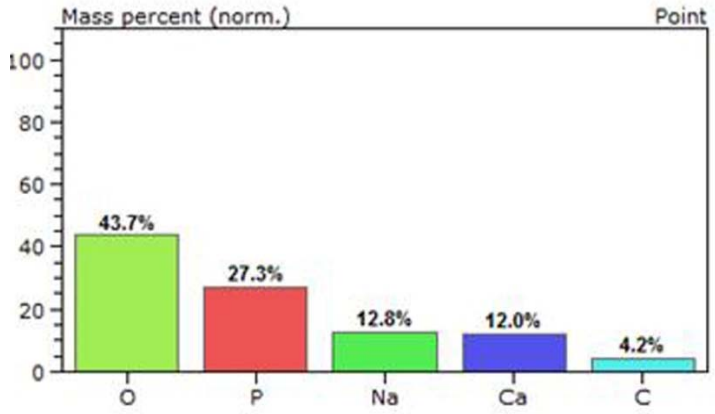

Fig.5. Mapping analysis of HA coating deposited on the surface of 316L stainless steel surface.

Table 1 shows porosity volume fraction and mean pores size in HA structure sintered at three different temperatures obtained by image analysis using the appropriate software. It is observed that by increasing the sintering temperature the mean pores volume fraction and the porosity size are decreased and a denser structure is obtained. The decrease in the porosity volume is considered to be useful for the improvement of mechanical strength of the material [26]. High sintering temperature results in reducing the coating biocompatibility and decomposition of the HA structure [28]. Since porous HA is more resorbable and osteoconductive than dense HA, the application of HA porous structure in the bone replacement can be considered as a suitable alternative [29].

Table 1. Porosity volume fraction and mean pores size obtained by image analysis.

Parameter	Stainless steel 316 L			Ti-6Al-4V		
Sintering temperature (°C)	600	700	800	600	600	800
Porosity volume fraction (%)	18.259	5.056	0.883	15.261	2.558	0.257
Pores mean size (μm)	19	6	< 1	20	2	< 1

Images obtained during 3D AFM analysis of the HA coating surface roughness after its deposition on 316L stainless steel and Ti-6Al-4V alloy specimen surface are presented in Fig. 6.

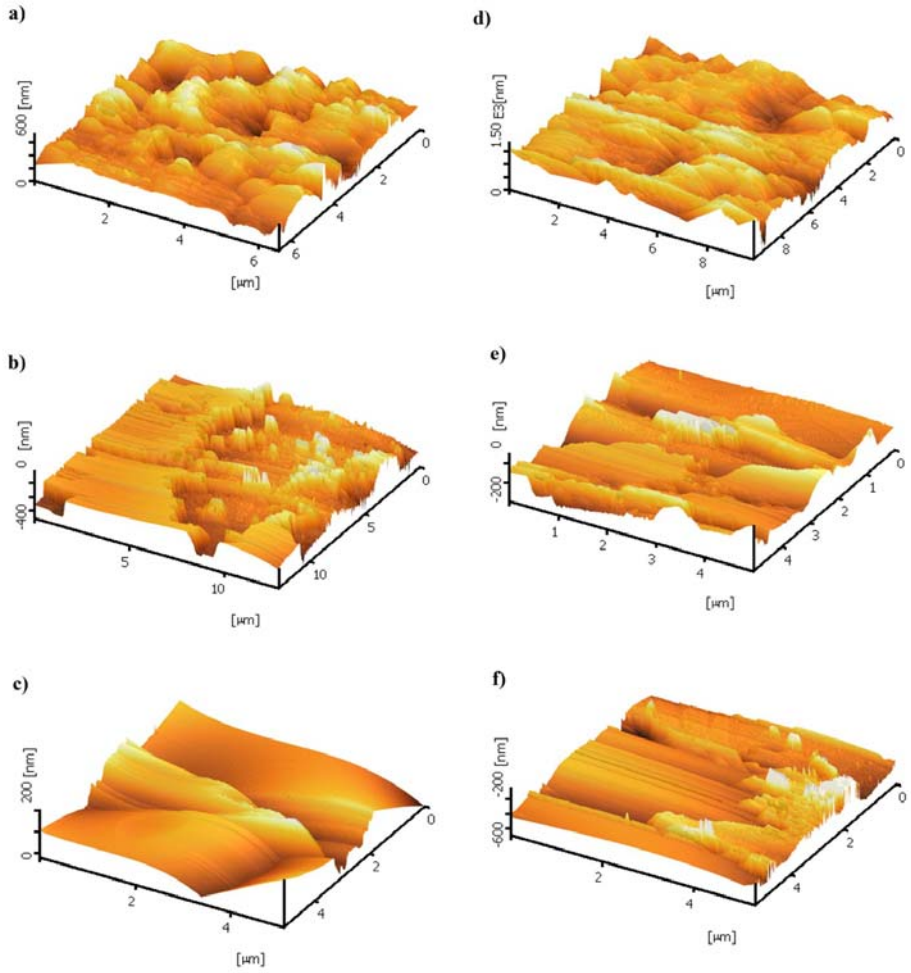

Fig.6. AFM 3D images of HA coating deposited on the substrates; 316 L stainless steel sintered at a) 600 °C, b) 700 °C, c) 800 °C and Ti-6Al-4V sintered at d) 600 °C, e) 700 °C, f) 800 °C.

Table 2 shows average roughness (R_a) and root mean square roughness (RMS) data measured by AFM technique. According to these results by increasing the sintering temperature the surface porosity is decreasing and HA grains begin to crystallize. By increasing the sintering temperature up to 700 ºC decrease in R_a and RMS values for both alloys and smoother surface is obtained. However, the alloys sintered at higher temperature (800 ºC) shows higher values of R_a and RMS. The surrounding tissue of the implants is mainly consisting of oxygen, water, proteins, negative and positive ions which further help to build structures like cells. Hence, the surface of the implant represents broken bond with higher surface energy. It is believed that surface energy of the surrounding tissue increases with increasing the sintering temperature, causing an immediate reaction to form new bonds. Therefore, surface properties of the implants

such as surface roughness and its morphology strongly influence cell proliferation, cell attachment and protein adsorption. [26]. It means that greater roughness cause exposure of more surface area for interaction with biomaterials. Therefore, it can be said that HA coating sintered at 600 °C shows optimum results in terms of interconnected porosity and surface roughness.

Table 2. Surface roughness parameters measured using AFM technique.

Parameter	316 L Stainless steel			Ti-6Al-4V alloy		
Sintering temperature (ºC)	600	700	800	600	700	800
Root mean square roughness (RMS)	78.89	36.14	36.21	167.4	43.82	47.45
Average roughness (R_a)	63.62	20.88	28.6	130.03	43.82	63.68

It is found that by applying withdrawal rate of 10 cm/min, maximum coating thickness of 50 µm can be obtained. Low dip and withdrawal rate of 5 cm/min results in thicker coating (100 µm and above), obtaining a cracked surface on the biomaterials. SEM micrograph, shown in Fig. 7(b), reveals presence of a gap between HA layer and the substrate, which causes a reduction in the bonding strength (see arrows). On the other hand, as it is shown in Fig. 7(a), presence of the gap in the thinner coating was not detected indicating that HA is bonded strongly to the substrate. Therefore, dipping and withdrawal rates control is an important factor in obtaining desirable coating thickness.

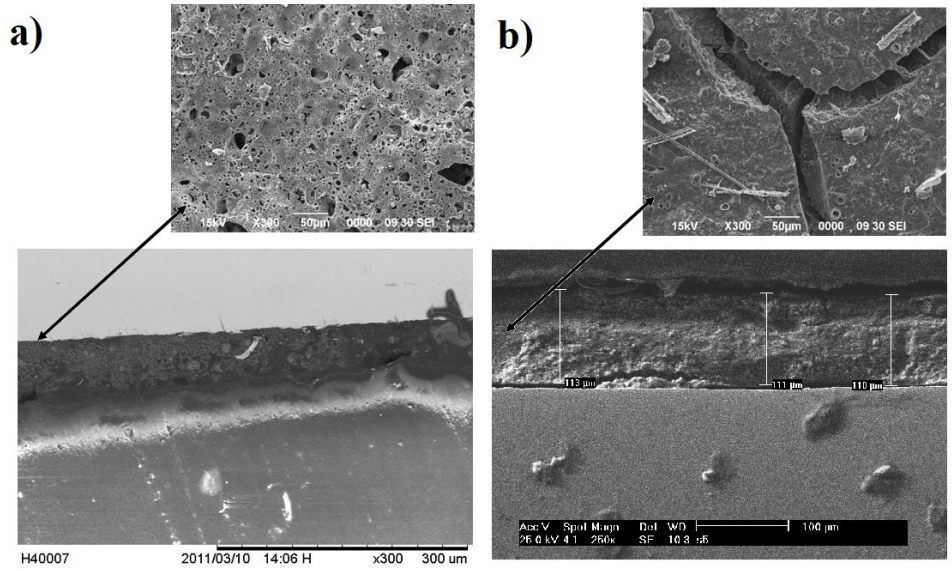

Fig.7. SEM micrographs showing cross section of sintered HA layer with thickness of a) 50 µm and b) 110 µm.

XRD patterns of deposited HA coating on Ti-6Al-4V alloy and 316L stainless steel surface are presented in Fig. 8. Some characteristic peaks of HA and porous tricalcium phosphate (TCP) phase is observed between 20 and 50 ° of 2θ. The peaks related to the CaO phase are appeared between 40-45 º and 55-60º of 2 θ. The strongest peak of HA is shown to be at 30º of 2θ. As seen from the XRD patterns, the increase in time and current density of electrodeposition resulted in a gradual improvement in crystallinity of the formed phases. Types of TCP compounds produced by the deposition were found to vary depending on the type and surface condition of the substrates and coating technique parameters. There is a gradual improvement of the peak sharpness of the HA phase with increase in sintering temperature. As revealed by XRD and DSC-TG analysis, at the higher sintering temperature, HA was more crystallized inducing some release of stress in the coating. The stresses were accommodated by viscous flow or diffusive creep as a result of high atomic mobility in the crystallization processes. The shift and crystallinity depression of HAP and TCP peaks indicate the presence of molecular interactions between HA and the substrates.

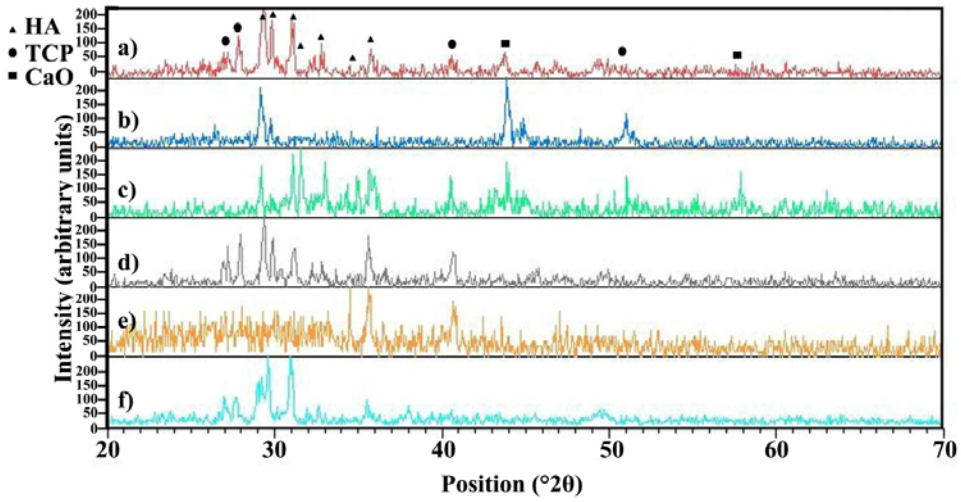

Fig.8. XRD patterns of HA coating deposited on the surface of 316L stainless steel sintered at a) 600 °C, b) 700 °C, c) 800 °C and Ti-6Al-4V alloy sintered at d) 600 °C, e) 700 °C, f) 800 °C.

Response of the HA coating to mechanical tests

Bonding strength of HA coating deposited on the surface of 316L stainless steel and Ti-6Al-4V alloy specimens sintered at three different temperatures is shown in Fig. 9. It is evident that by increasing the sintering temperature, the bonding strength of the specimens is increased except for the titanium alloy sintered at 800 °C due to the presence of cracks. The presence of pores in the HA layer sintered at 600 °C for both substrates lead to the lower bonding strength. By increasing the sintering temperature denser structure of HA is obtained, resulting in higher bonding strength. It is found that HA coating on the stainless steel sintered at 800 °C showed highest value of bonding

strength (~27 MPa) while lowest bonding strength value (~10 MPa) was detected for Ti-6Al-4V alloy specimens sintered at 800 °C.

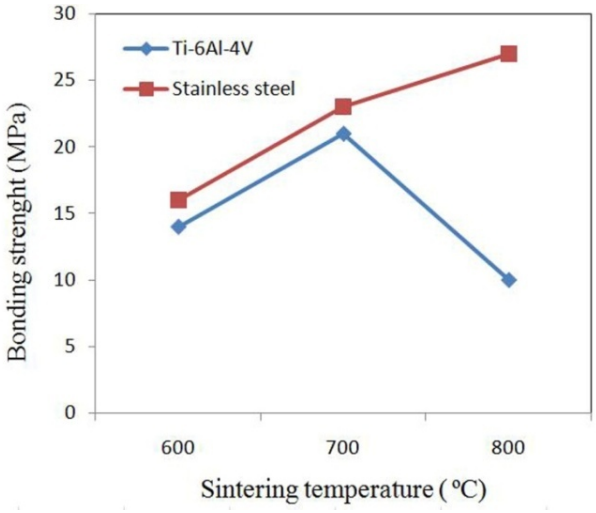

Fig.9. Bonding strength of the specimens sintered at different temperatures.

In Fig. 10 results of microhardness measurements of the coated substrates are shown. The hardness of the HA coating deposited on the surface of examined substrates is enhanced with the increase of the sintering temperature. However, as can be seen from the microhardness profiles, the microhardness values of the deposited coating on the titanium alloy in all sintering temperatures are lower than the deposited layer on the stainless steel due to the presence of the cracks on the surface of the alloy.

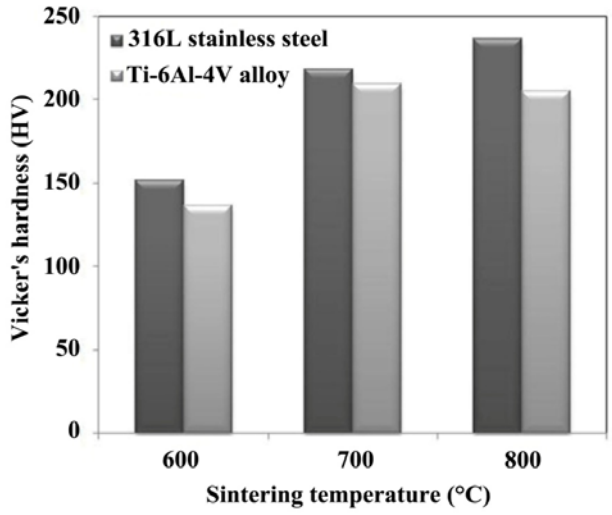

Fig.10. Microhardness of the coated specimens subjected to different sintering temperatures.

Conclusion

Sol-gel dip coating method is proved to be a cheap and easy coating deposition method for the metallic biomaterials. The coating deposition repeatability and the deposited coating quality can be altered by changing the coating deposition parameters. The important findings of this work are as follows:

1. When the coating thickness reaches 50 μm, cracks appear on the surface of the coated specimen surface. The most important factors of the coating thickness control are find to be withdrawal rate, immersion time and sol-gel solution viscosity.

2. It was observed that by increasing the sintering temperature denser HA layer can be obtained. Porosity volume fraction and mean pores size are decreasing by increasing the sintering temperature.

3. At the higher sintering temperature, surface of the deposited HA was cracked resulting in decreasing mechanical properties of the coating layer on the titanium alloy.

4. Higher surface roughness at the lower sintering temperature (600 ºC), causes more contact are between the coating surface and biomaterials. Surface roughness of the HA coating deposited on Ti-6Al-4V alloy specimens was more pronounced than in the case of HA layer deposited on the surface of 316L stainless steel specimens.

Acknowledgment

The authors are grateful to the Universiti Teknologi Malaysia and Dr. Zameri for financial support of this project.

References

[1] A. Balamurugan , S. Kannan, S. Rajeswari, Evaluation of TiO_2 coatings obtained using the sol–gel technique on surgical grade type 316L stainless steel in simulated body fluid, Materials Letters 59 (2005) 3138-3143.

[2] C. Garcia, S. Cere, A. Duran, Bioactive coatings prepared by sol–gel on stainless steel 316L, Journal of Non-Crystalline Solids 348 (2004) 218-224.

[3] L. Guo, H. Li. Fabrication and characterization of thin nano-hydroxyapatite coatings on titanium, surface & Coatings Technology 185 (2004) 268-274.

[4] J. Harle, H.W. Kim, N. Mordan, J.C. Knowles, V. Salih, Initial responses of human osteoblasts to sol–gel modified titanium with hydroxyapatite and titania composition, Acta Biomaterialia 2 (2006) 547-556.

[5] K. Chenga, S. Zhanga, W. Weng, X. Zeng, The interfacial study of sol–gel-derived fluoridated hydroxyapatite coatings, Surface & Coatings Technology 198 (2005) 242-246.

[6] V. Deram, C. Minichiello, R.N. Vannier, A. Le Maguer, L. Pawlowski, D. Murano, Microstructural characterizations of plasma sprayed hydroxyapatite coatings, J Surface and Coatings Technology, 166 (2/3) (2003) 153-159.

[7] M. Mazar Atabaki, J. Rabi'atuladawiyah, J. Idris, Sol-gel bioactive glass coating for improvement of biocompatible human body implant, Metalurgija, 6(3) (2010) 49-163.

[8] P.A. Ramires, A. Romito, F. Cosentino, E. Milella, The influence of titania/hydroxyapatite composite coatings on in vitro osteoblasts behavior, Biomaterials 22 (2001)1467-1474.

[9] K. De Groot, R.G.T. Geesink, C.P.A.T. Klein, P. Serekion, Plasma sprayed coatings of hydroxylapatite. J. Biomed Mater Res., 21 (1987) 1375-81.

[10] A.E. Porter, L.W. Hobbs, R.V. Benzra, The ultrastructure of the plasma-sprayed hydroxyapatiteübone interface predisposing to bone bonding, Biomaterials, 23 (3) (2002) 725-733.
[11] Y.P. Lu, M.S. Li, Z.G. Wang, Plasma-sprayed hydroxyapatite+titania composite bond coat for hydroxyapatite coating on titanium substrate, Biomaterials, 25 (18) (2004) 439-440.
[12] S.J. Ding, C.P. Ju, L.J.H. Chern, Characterization of hydroxyapatite and titanium coatings sputtered on Ti-6Al-4V substrate, J. Bio-medicine Mater. Res., 44 (3) (1999) 266-279.
[13] J.E.G. Hulshof, K. van Dijk, J.P.C.M. van der Waerden , J.G.C. Wolke, L.A. Ginsel , J.A. Jansen, Biological evaluation of the effect of magnetron sputtered Ca/P coatings on osteoblast-like cells in vitro. J. Biomed Mater. Res., 29 (1995) 967-975.
[14] M. Wei, AJ. Ruys, B.K. Milthorpe, C.C. Sorrell, Solution ripening of hydroxyapatite nanoparticles: effects on electrophoretic deposition. J Biomed Mater. Res., 45 (1999) 11-19.
[15] P, Ducheyne, W, Van Raemdonck, J.C. Heughebaert, M. Heughebaert, Calcium phosphate ceramic coatings on porous titanium: effect of structure and composition on electrophoretic deposition, vacuum sintering and in-vitro dissolution, Biomaterials, 11 (1990) 244.
[16] Z. Xuhui, Y. Lingfang, Z. Yu, X. Jinping, Hydroxyapatite Coatings on Titanium Prepared by Electrodeposition in a Modified Simulated Body Fluid, Chinese Journal of Chemical Engineering, 17 (3) (2009) 667-671.
[17] C.T. Kwok , P.K. Wong , F.T. Cheng , H.C. Man, Characterization and corrosion behavior of hydroxyapatite coatings on Ti6Al4V fabricated by electrophoretic deposition, Applied Surface Science 255 (2009) 6736-6744.
[18] I.M.O. Kangasniemi, C.C.P.M. Verheyen, E.A. van der Velde, K. de Groot, In vivo tensile testing of flouoroapatite and hydroxylapatite plasma-sprayed coatings. J. Biomed Mater. Res. 28 (1994) 563-72.
[19] W. Xu, W. Hu, M Li, C. Wen, Sol-gel derived hydroxyapatite/titania biocoatings on titanium substrate, Materials Letters, 60 (2006) 1575-1578.
[20] D. Wang, G.P. Bierwagen, Sol-gel coatings on metals for corrosion protection, Progress in Organic Coatings, 64 (2009) 327-338.
[21] H.W. Kim, Y.M. Kong, C.J. Bae, Y.J. Noh, H.E. Kim, Sol-gel derived fluor-hydroxyapatite biocoatings on zirconia substrate, Biomaterials, 25 (2004) 2919-2926.
[22] M.F. Hsieh, L.H. Perng, T.S. Chin, Hydroxyapatite coating on Ti6Al4V alloy using a sol-gel derived precursor, Materials Chemistry and Physics, 74 (2002) 245-250.
[23] D.M. Liu, T. Troczynski, W.J. Tseng, Water-based sol-gel synthesis of hydroxyapatite: process development, Biomaterials, 22 (2001) 1721-1730.

[24] H.W. Kim, Y.H. Koh, L.H. Li, S. Lee, H.E Kim, Hydroxyapatite coating on titanium substrate with titania buffer layer processed by sol-gel method, Biomaterials, 25 (2004) 2533-2538.
[25] B. Aksakal, C. Hanyaloglu, Bioceramic dip-coating on Ti-6Al-4V and 316L SS implant materials, J. Mater. Sci. Mater. Med., 19 (2008) 2097-2104.
[26] S.R. Paital, N.B. Dahotre. Calcium phosphate coatings for bio-implant applications: Materials, performance factors, and methodologies, Materials Science and Engineering R, 66 (2009) 1-70.
[27] H. Petite, V. Viateau, W. Bensaid, A. Menunier, C.D. Pollak, M. Bourguignon, K. Ourdina, L. Sedel and G. Guillemin, Tissue-engineered bone regeneration, Nature tech., 18(2009) 959.
[28] J. Ma, C.H. Liang, L.B. Kong, C. Wang, Colloidal characterization and electrophoretic deposition of hydroxyapatite on titanium substrate, journal of materials science: materials in medicine, 14 (2003) 797-801.
[29] C.A. Leony Leon, New perspectives in mercury porosimetry, Adv. Colloid Interface Sci., (1998) 76-77.